1990 SCA CONFERENCE PAPER NUMBER 9005

Pore Volume Compressibilities under Different Stress Conditions

Ziqiong Zheng, John McLennan, and Arfon Jones
Terra Tek, Inc.
Salt Lake City, Utah

ABSTRACT

Pore Volume Compressibilities were determined for reservoir rocks at different in-situ conditions representative of reservoir drawdown. Such conditions are simulated in the laboratory by subjecting a reservoir rock sample to virgin in-situ conditions as described by the overburden stress, average lateral stress, pore pressure and temperature, followed by pore pressure drawdown. During pore pressure drawdown, zero lateral deformation (representing horizontal restraint) and constant axial stress (representing constant overburden) are maintained.

Pore volume compressibilities for sandstone were measured under simulated in-situ conditions and hydrostatic compression (conventional). The results show the pore volume compressibilities measured under the two conditions can differ by as much as a factor of two. This can have significant impact on designing reservoir management strategies.

Based on the assumption that the rock bulk and the pore system deform elastically, the relationships between pore volume compressibilities measured at simulated drawdown conditions with other conventional methods, as well as the relationship to different compressibilities are presented in the paper. In addition the experimental methods used will be described.

Modification of the reservoir effective stress by virtue of production impacts the volumetric changes in pore spaces in a reservoir. The engineering parameters quantifying these volumetric variations are compressibilities. The application of reliable compressibility includes reservoir pressure maintenance and subsidence evaluations (Ruddy et al., 1989; Johnson et al., 1989; Geertsma, 1973). Production forecasting is intimately related to a total system compressibility combining the saturation weighted compressibilities of liquid and gaseous phases in the pore space and the pore volume compressibility, often referred to as formation compressibility. Correlations are often used (Hall, 1953). These, although readily applicable, may be in error by an order of magnitude (Earlougher, 1977). Correlations such as this as well as certain laboratory determinations are applied with risk largely because of poor appreciation of the mechanics of compressibilities and the stress paths during laboratory testing.

For formations that will be subject to nonlinear elastic or inelastic pore deformation with changes in reservoir pressure, there is need to determine its pore compressibility along pressure/strain history paths encountered during production and water injection (flooding).

Three types of compressibilities are often cited in characterization of a porous medium. There is Bulk Compressibility, C_b, representing the relative changes in bulk volume of the medium; Solid (Grain) Compressibility, C_s, describing the relative changes in the solid portion of the medium; and, Pore Volume Compressibility, C_p, describing relative changes in pore volume.

The most often used definitions of compressibility are as follows:

$$C_{bc} = \frac{-1}{V_b}\left(\frac{\partial V_b}{\partial P_c}\right)_{P_p} \quad and \; C_{bp} = \frac{1}{V_b}\left(\frac{\partial V_b}{\partial P_p}\right)_{P_c} \tag{1}$$

$$C_{pc} = \frac{-1}{V_p}\left(\frac{\partial V_p}{\partial P_c}\right)_{P_p} \quad and \; C_{pp} = \frac{1}{V_p}\left(\frac{\partial V_p}{\partial P_p}\right)_{P_c} \tag{2}$$

$$C_{sc} = C_{sp} = \frac{-1}{V_b}\left(\frac{\partial V_b}{\partial P_c}\right)_{P_p} = \frac{1}{V_p}\left(\frac{\partial V_p}{\partial P_p}\right)_{P_c}, \; (d(P_c - P_p) = 0) \tag{3}$$

where:

- subscript b denotes bulk volume,
- subscript p represents pore pressure or pore volume,
- subscript c indicates confining pressure is applied,
- subscript s denotes solid volume (grain portion of the rock),

- P_c and P_p denote confining and pore pressure, respectively, and,
- Subscript outside of parenthesis indicates the pressure to be maintained constant.

In the foregoing equations, the first subscript indicates the volume component of interest, while the second indicates the pressure/stress causing the relative volume change.

The interrelationship between all of the above compressibilities can theoretically be derived based on stress conditions and constraints, Zimmerman (1986), for example, derived such relationships:

$$C_{bp} = C_{bc} - C_{sc} \tag{4}$$

$$C_{pc} = (C_{bc} - C_{sc})/\phi \tag{5}$$

$$C_{pp} = [C_{bc} - (1+\phi)C_{sc}]/\phi \tag{6}$$

where ϕ is the sample porosity.

The two bulk compressibilities, (C_{bc} and C_{bp}), and grain compressibility ($C_{sc} = C_{sp}$) are measured directly from specimen volumetric deformation. Pore compressibility (C_p), the fundamental compressibility from a production perspective, can only be determined indirectly through measurement of volume changes of the pore fluid. Therefore, the measurement of C_p is complicated by a number of factors. These include the compressibility of the pore fluids, the degree of saturation, the pore space connectivity, the morphology, distribution and aspect ratio of the pore structure and the compressibility of the test system. To minimize the effect of these factors and to simplify testing procedures, most routine industrial pore volume compressibility measurements are performed by subjecting a sample to hydrostatic compression with constant pore pressure, usually atmospheric pressure (so that no pore fluid compressibility problem is involved). This is a special case of C_{pc}:

$$C_{pc} = \frac{\partial V_p}{V_p \partial P_c}, \ (P_p = 0, \text{ or constant}) \tag{7}$$

or even more simplified,

$$C_{pc} = \frac{\partial V_b}{V_b \partial P_c}, \ (P_p = 0, \text{ or constant}) \tag{8}$$

The latter equation implies the common assumption that the grain compressibility, which is large in many shales, is zero. Unfortunately, such testing does not reliably reflect the in-situ conditions which reservoir rock, would encounter. During production, *the reservoir (pore) pressure decreases from an initial pressure (not atmospheric pressure). The stress due to overburden (total vertical stress) does not change, and, the lateral deformation is constrained by the earth's crust. These conditions are greatly different from the routine C_{pc} measurement conditions described above.* Recognizing compressibility dependence on stress path and in-situ conditions during production, pore volume compressibility measurements on conventional reservoir rocks are increasingly performed under uniaxial strain conditions. That is, the total vertical stress (overburden) and lateral strain are maintained constant during pore pressure changes (drawdown). Specifically:

$$C_{pu} = \frac{\partial V_p}{V_p \partial P_p} \; and \; d\sigma_1 = d\epsilon_t = 0 \tag{9}$$

where:

- $d\sigma_1$ is the variation in total vertical stress,
- $d\epsilon_t$ is the variation lateral strain (deformation), and
- Consistent with previous nomenclature, the second subscript indicates uniaxial strain and constant vertical stress.

  Although uniaxial strain conditions are unquestionably more appropriate, uncertainties remain and data interpretation is complex.

All of the above compressibilities, except C_{pu}, are defined in terms of uniformly distributed stresses. The compressibility measured under production conditions (C_{pu}), however, can not be readily related to other compressibilities measured under hydrostatic conditions due to the deviatoric stress involved in this condition. The discussion section of this paper will demonstrate such effects.

LITERATURE REVIEW

Terzaghi (1936) performed experiments under hydrostatic conditions with sand, clay and concrete. He concluded from these experiments that the difference between the confining pressure and the pore fluid pressure was "effective" in controlling changes in bulk volume. This "effective" stress is simply the difference between the applied external stress and pore pressure. Biot (1941) developed the theory for the mechanical behavior of porous materials based on energy conservation principles and introduced the concept that the "effective" stress should be the difference between the confining stress and a portion of the pore pressure. Biot's coefficient, the correction factor for the portion of pore pressure, has been commonly used in poroelasticity. Geertsma (1957) derived relationships between the different compressibilities, assuming material isotropy, homogeneity and linear elasticity. Van der Knaap (1959) extended Geertsma's work and calculated the correction factor for effective stress for non-linear stress-strain relationships. Rice and Cleary (1976) formulated equations for several boundary value problems, assuming quasi-static deformation of the porous material. Zimmerman et al. (1986) rederived the relationships between different compressibilities and effective stress coefficients[1]. They also derived upper and lower bounds of ratios between different compressibilities. Fundamental studies have been carried out in determining compressibility of linear elastic and nonlinear elastic materials under hydrostatic stress conditions. These concepts have yet to be routinely applied in the petroleum industry.

EXPERIMENTATION

To qualify the loading path sensitivity and to determine compressibilities for reservoir design and simulation, two groups of relatively unconsolidated sandstones were subjected to different loading path regimes. The three sets of twin samples from Group A were subjected to both hydrostatic compression and simulated production conditions (pore pressure drawdown under constant axial stress and zero lateral strain) whereas the four samples from Group B were only tested under simulated production conditions (Refer to Table 1).

Sample Selection and Preparation

To eliminate factors that can add uncertainties to the interpretation of results, the locations of core plugs for testing from the provided core were selected after CT scanning. The samples were chosen at locations of most uniformity on CT scan graph, which indicates consistent density. At each location of interest, twin samples were cored, cut and endground parallel to within a tolerance of ± 0.001 inch. To avoid any uncertainty due to multiple phase pore fluid in the sample (original pore fluid and saturation fluid for the test), Dean Stark cleaning procedure was used to clean the original formation fluid from the sample. Each sample was then fully saturated by brine .

Measurement of Compressibility under Hydrostatic Stress

Pore volume compressibility was measured on one of the twin samples from Group A under progressively increasing net hydrostatic compressive stress. This is the most commonly used method in petroleum engineering to determine pore volume compressibility as a function of effective stress.

The hydrostatic confining stress was raised in steps of different intervals and the changes of pore volume in the sample (in this measurement, the pore pressure was maintained at atmospheric level) were measured. Sample deformation was not measured.

[1] Many other references on poroelasticity exist; for example, Fatt, 1958; Bhatt et al., 1975; Yew and Jogi, 1978; Zimmerman, 1984, 1985; Ricnicki, 1985; Detournay and Cheng, 1988 ...

Table 1: Sample Description and Test Matrix

Group	Sample	Description	E* (10^6 psi)	ν*	Hydrostatic Compression	Production Simulation
A	A-1	Well indurated, well sorted, medium-grained (300–500 μm) quartz sandstone.	1.23	.18	•	•
A	A-2	Well indurated, well sorted, fine-grained (150–180μm) quartz sandstone.	2.18	.27	•	•
A	A-3	Poorly indurated, moderate to well sorted, coarse grained (500–μm) quartz sandstone.	0.70	.05	•	•
B	B-1	Moderately indurated, poorly sorted, fine-grained sandstone (55% quartz).	2.59	.19		•
B	B-2	Moderately indurated, moderately sorted, medium-grained sandstone (75% quartz).	N/A	N/A		•
B	B-3	Poorly indurated, moderately to poorly sorted, fine to medium-grained sandstone (85% quartz).	1.42	.13		•
B	B-4	Well indurated, well sorted, very fine to fine-grained sandstone (85% quartz).	2.28	.19		•

* These mechanical properties were measured after pore pressure drawdown, hence they are "post-production" elastic modulus and Poisson's ratio.

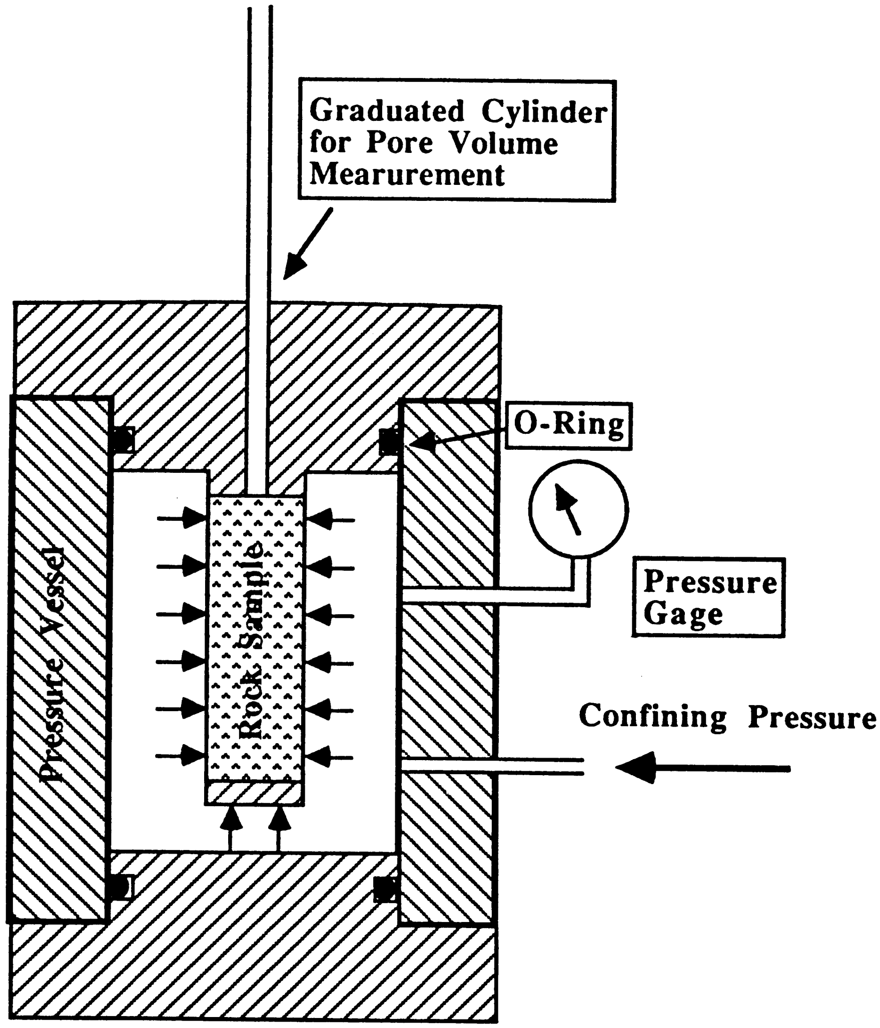

Figure 1: Schematic measurement system for hydrostatic compression

Under Simulated In-Situ Production

Samples from Groups A and B were subjected to pore pressure drawdown under uniaxial strain conditions.

Prior to testing, each sample was assembled with strain and pore volume measurement instrumentation. The sample was sandwiched between two endcaps with radial and circumferential grooves to accommodate pore fluid displacement to and from the pore fluid accumulator. The sample and endcaps were sealed in an impermeable membrane preventing invasion by the confining fluid. The strain measurement system was an extremely accurate strain-gaged cantilever system.

Each sample was put into a pressure vessel, capable of providing a confining pressure up to 30,000 psi. A vacuum pressure of $\sim$ 50 psi was applied to the entire system for 12 hours. This was followed by backflooding with brine. The "virgin" bench permeability was measured by flowing the same brine through the sample. The stresses on the sample were first raised to assumed in-situ stress levels (axial stress was applied to simulate overburden stress, lateral confining stress was applied to simulate

an average horizontal stress and pore pressure was applied to simulate the initial reservoir pressure), these pressure and stress levels were maintained constant to allow equilibration of all strains. At this point, the sample is subjected to simulated pre-production in-situ conditions. After strain equilibrium was reached pore pressure drawdown was started to simulate production. During the entire production simulation, the axial stress and lateral strain were held constant to simulate constant overburden and horizontal constraint. As the pore pressure is reduced, the confining pressure was reduced via computerized servo-control to maintain constant lateral strain. A pore pressure drawdown rate of -0.1 psi/sec was used in 100 psi intervals from 4800 psi to 4000 psi to simulate initial production to waterflooding, and in 400 psi intervals from 4000 psi to 2000 psi to simulate waterflooding to well abandonment. At the end of each pore pressure drawdown interval, a holding period was applied to allow strain equilibrium.

Figure 2 shows the pore pressure drawdown schedule for the tests. Throughout the entire test, the fluid volume change in the accumulator, which represent the change in sample pore fluid volume, was measured.

RESULTS AND DISCUSSION

Figure 3 shows the changes in porosity for samples A-1, A-2, and A-3, calculated from the measured changes in pore volume during progressively increasing effective hydrostatic confining stress application. The pore volume compressibility shown in Figure 4 was calculated using equation 7. The general trend in changes of compressibility is as expected. Notice the

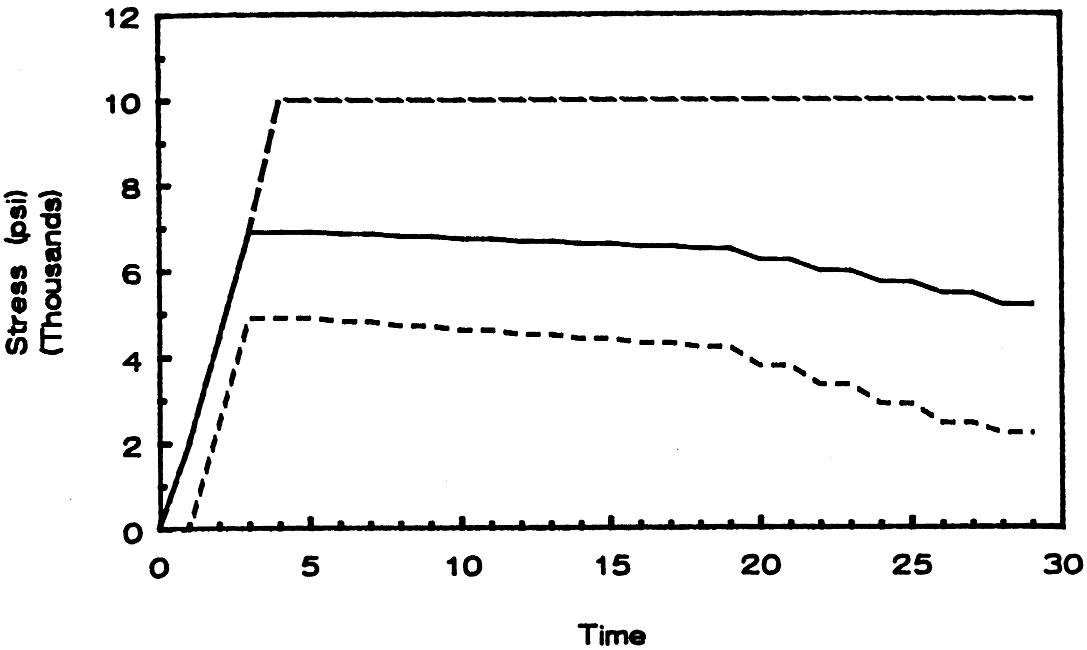

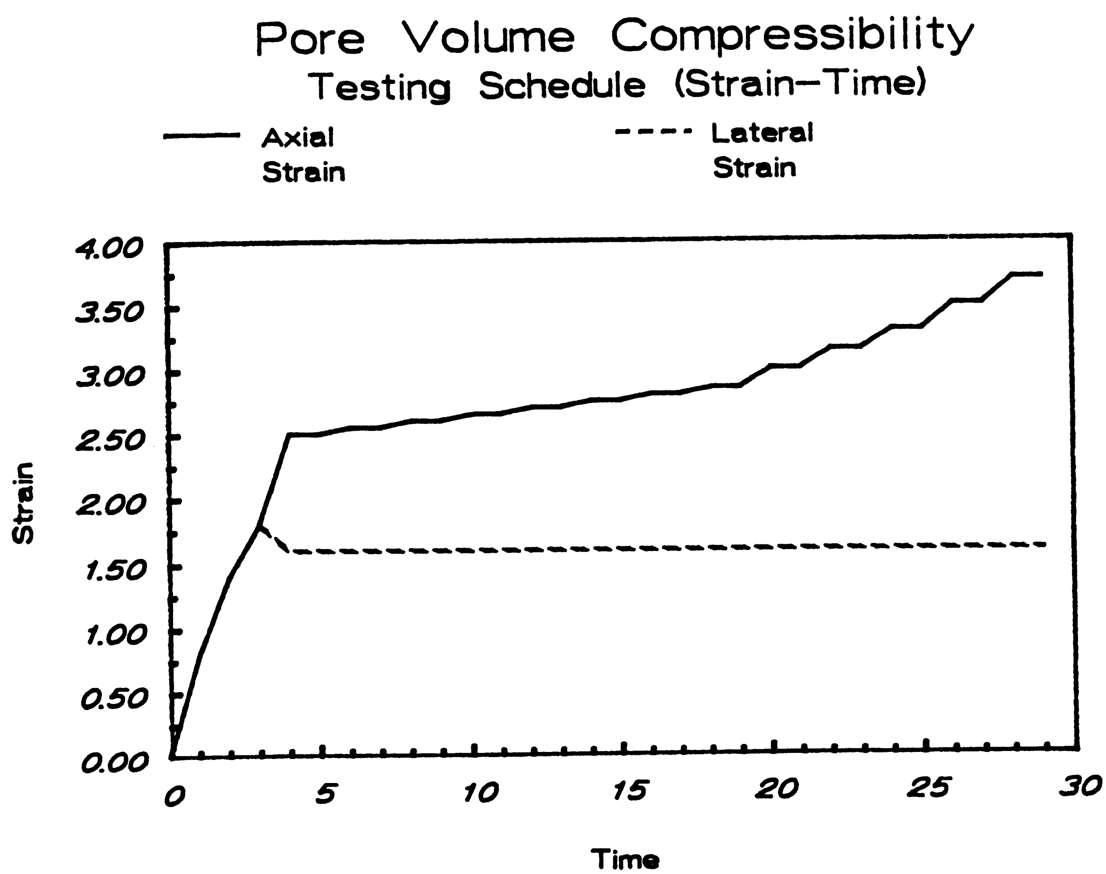

Figure 2: Testing Schedule Under Simulated Production Conditions

large fluctuation in pore compressibility and porosity at a confining stress level of 5,000 to 6,000 psi. Though the samples were not examined microscopically, it is expected that this large fluctuation is due to onset of to the collapse of pore space.

Table 2 shows the pore volume compressibilities measured under simulation production conditions for Group A. Samples A-1 and A-2, showed an increase in pore volume compressibility as the pore pressure was reduced (and that the effective confining stress and deviatoric stress are increased), instead of a decrease as exhibited by sample A-3. Similar behavior to A-1 and A-2 was manifest by sample B-4. Figure 5 shows the changes of pore compressibility, calculated from equation 9, as a function of pore pressure.

Table 2: Measured Compressibilities

Group	Sample	Initial Porosity (%)	Pore Pressure Range (psi)	Pore Volume Compressibility (10^{-6} psi^{-1})	
				Hydrostatic Compression	Simulated Production
A	A-1	32.24	4880–4200	30	21.7
A	A-2	12.04	"	8*	21.2
A	A-3	25.25	"	30	37.5
A	A-1	32.24	4200-2000	21	39.5
A	A-2	12.04	"	6*	28.9
A	A-3	25.25	"	22	30.4
B	B-1				
B	B-2				
B	B-3				
B	B-4				

* The sample tested in hydrostatic compression has a very low porosity, which is about half of all other samples tested both under hydrostatic conditions and simulated production.

As these tests apply different stress conditions to the samples, it is important to contrast the measurements at an identical stress condition. One means of doing this is to use the effective mean stress, σ'_{mean}:

$$\sigma'_{mean} = \frac{\sigma_1 + \sigma_2 + \sigma_3}{3} - \alpha P_p \qquad (10)$$

where α is the Biot's poroelastic coefficient for pore pressure correction. At equivalent effective mean stresses, hydrostatic and simulated production methods showed substantial

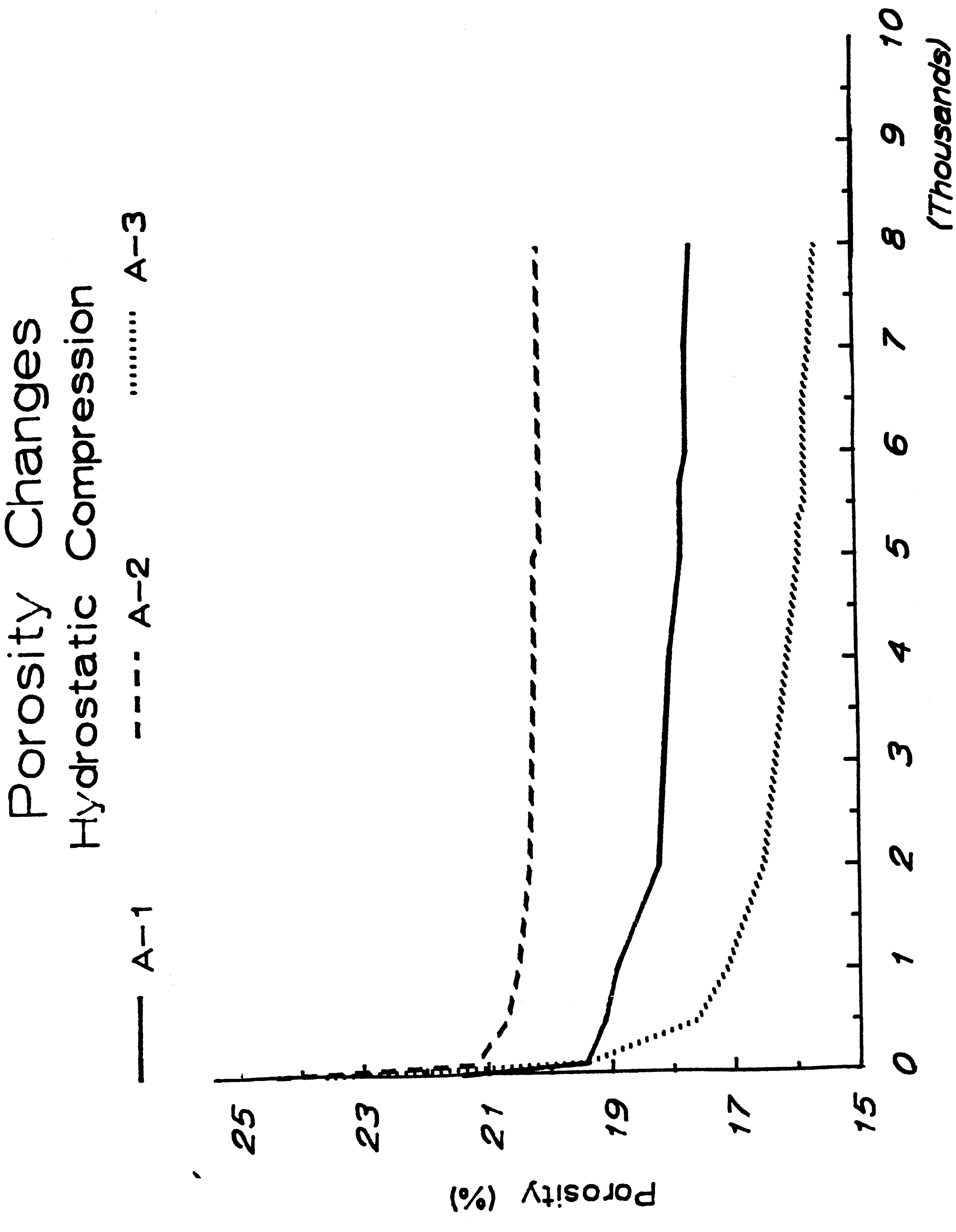

Figure 3: Porosity as a function of hydrostatic confining stress

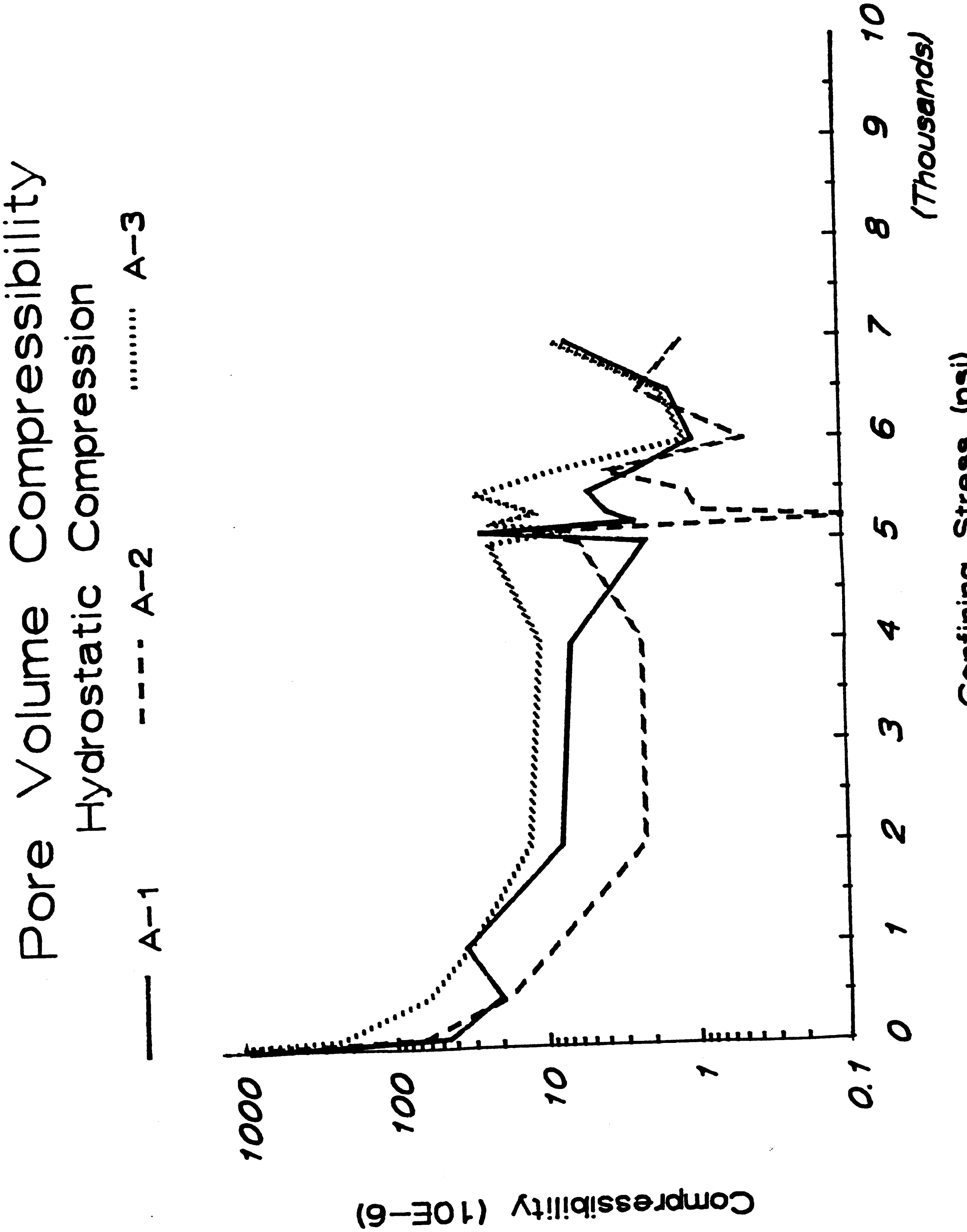

Figure 4: Pore volume compressibility under hydrostatic confining stress

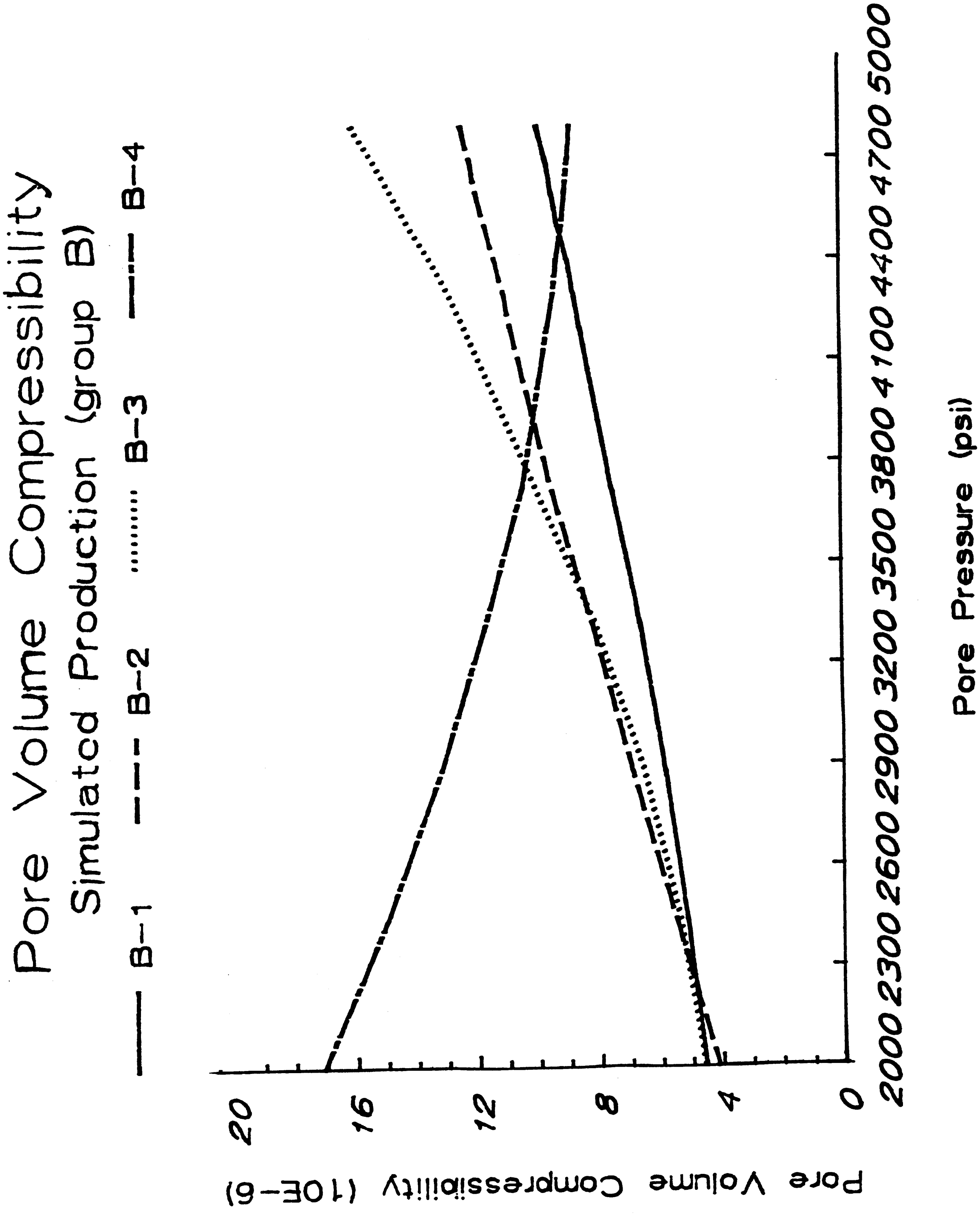

Figure 5: Pore volume compressibility (under simulated production) as a function of pore pressure

differences (up to a factor of 2). For example, in an effective mean stress range of 3,000 to 4,000 psi, the pore volume compressibility from simulated production was almost twice that determined using hydrostatic compression alone. However, the theoretical derivation shown below suggests that one would anticipate the opposite ($C_{pc} > C_{pu}$):

Presume that $$d\sigma_1 = d\epsilon_t = 0 \tag{11}$$

$$\sigma'_{mean} = \tfrac{1}{3}(\sigma_1 + 2\sigma_c) - \alpha P_p \tag{12}$$

$$C_{pu} = \frac{1}{V_p}\frac{\partial V_p}{dP_p} = \frac{1}{V_p}\frac{\partial V_p}{\partial \sigma'_{mean}}\frac{d\sigma'_{mean}}{dP_p} \tag{13}$$

and $$d\sigma'_{mean} = \frac{2}{3}\frac{d\sigma_c}{dP_p} - \alpha \tag{14}$$

therefore $$C_{pu} = \left\{\alpha - \tfrac{2}{3}k\right\} C_{pc} \tag{15}$$

where:

- C_{pc} – is as defined by equation 2.
- σ_{mean} – mean effective stress.
- k = $\frac{d\sigma_c}{dP_p}$ - variation of confining stress as a function of pore pressure (inverse of Skempton's parameter, B).
- α – Biot's poroelastic coefficient, α equals 1 for highly permeable porous mediums such as friable sandstone.

Some of the discrepancies are due to the fact that under conditions of simulated production, pore pressure is not atmospheric (even if mean effective stress levels are equal in the two methods). Furthermore, under conditions of simulated production, substantial deviatoric stress of $\sigma_1 - \sigma_3 = \sigma'_1 - \sigma'_3$ will cause permanent deformation, microfracture closure, shear fractures not possible under hydrostatic conditions.

Further anomalies, and cause for careful consideration of laboratory testing techniques is that samples A-1, A-2 and B-4, tested under simulated production conditions show an **increase in pore volume compressibility with increasing effective stress.** This behavior relates to the generation of microfractures and largely to pore collapse with increasing effective stress as the pore pressure is reduced during production. Consider the schematic model shown in Figure 6 (stress-strain history).

In region I (Figure 6), the effective stress is low and strains are relatively large, corresponding to the closure of voids with large aspect ratios (such as microcracks and bedding). Once the sample has been loaded to large effective stress representing in-situ stress conditions, most rocks are beyond this region of stress-strain behavior. Region II corresponds to the linear behavior of rock grains and pore spaces. All of the deformation is recoverable in this stress-strain range. An increase in effective stress results in a stiffening of the pores so that the pore compressibility decreases as the effective stress is increased. Most reservoir rocks

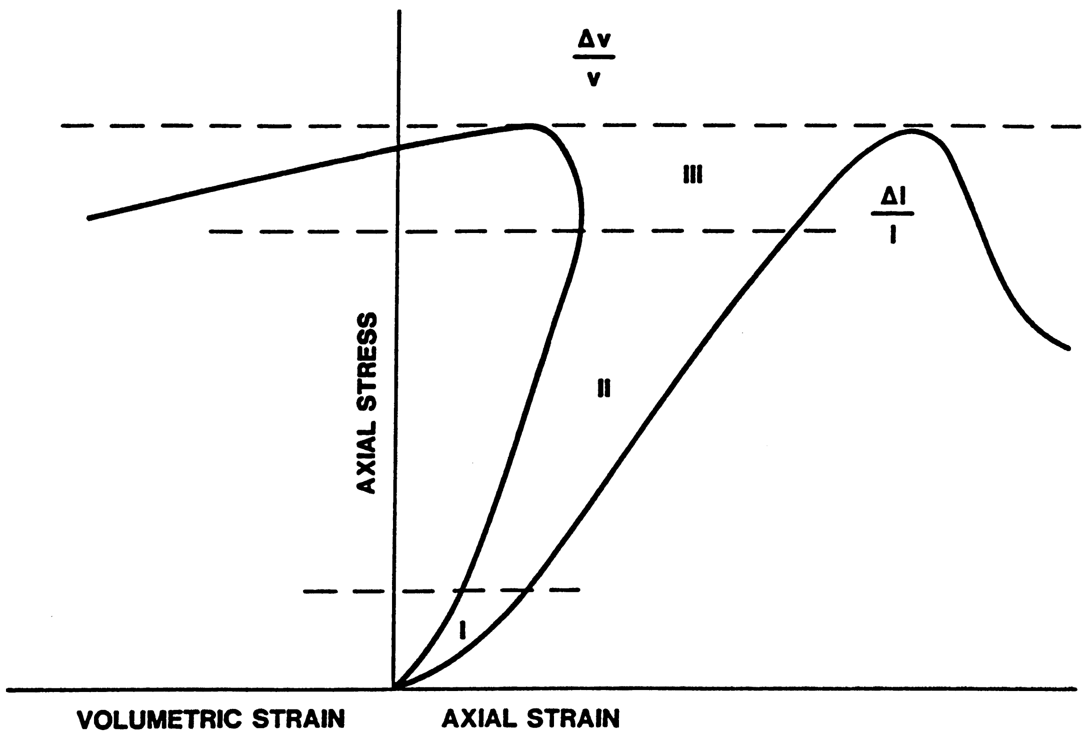

Figure 6: Stress-strain curve for a porous rock

are in this stress-strain region under virgin in-situ stress conditions (from estimated in-situ stress values and laboratory stress-strain relationship). In region III, non-linear stress-strain behavior corresponds to the generation of new microcracks and pore collapse. An increase in effective stress, as would happen with drawdown, can result in pore collapse and corresponds to an increase in pore compressibility, **if this compressibility is calculated from the pore fluid coming out of the sample when pore pressure is reduced.** Due to pore collapse, however, whether the term "compressibility" can still be appropriately used is an interesting question. Some rocks at undisturbed or virgin in-situ conditions, may be near failure already. Any increase in effective stress (due to reduction of pore pressure) will result in pore collapse and generation of microcracks. Samples A-1, A-2 and B-4 may be examples.

CONCLUSIONS

Conventionally measured pore volume compressibilities using effective stress (hydrostatic compression) method should not be used directly for reservoir characterization and life estimation. Due to the deviatoric stress applied on the sample during production, pore volume compressibility measured under simulated production conditions is more representative for reservoir characterization. Currently available data is insufficient to conclude if any reliable theoretical or empirical relationships exist between conventional hydrostatic measurements and simulated production measurements. During production, the increasing effective mean stress and deviatoric stress can cause pore collapse, and microcrack closure may result in an increase in pore volume compressibility. Such behavior in a reservoir may be indicative of the state of in-situ stress relative to the mechanical properties of the rock. Pore volume compressibility is a function of effective stress, as is commonly accepted, but is also a function of the absolute pore pressure value. Considering pore volume compressibility as a function of effective stress only could introduce significant errors in pertinent reservoir engineering calculations.

REFERENCES

1. Ruddy, I., Anderson, M.A., Patillo, P.D., Bishlawi, M., and Foged, N., *JPT*, 741-746, 1989.

2. Johnson, J.P., Rhett, D.W., and Siemers, W.T., *JPT*, 717-722, 1989.

3. Geertsma, J., *JPT*, 734-744, 1973.

4. Hall, H., *Trans. AIME*, Vol. 198, 309-311, 1953.

5. Earlougher, R.C.Jr., *Monograph V.5., Henry L. Soherty Series, SPE*, 1977.

6. Zimmerman, R.W., Somerton, W.H., and King. M.S., *JGR.*, Vol. 91, B12, 12765-1277, 1986.

7. Terzagh, K., *Proceeding of Int. Conf. Soil Mech. and Foundation Engineering*, 54-56, 1936.

8. Biot, M.A., *J. Appl. Phys.*, 12, 155-164, 1941.

9. Geertsma, J., *Trans. AIME*, 210, 331-340, 1957.

10. Van der Knapp, W., *Trans. AIME*, 216, 179-187, 1959.

11. Rice, J.R., and Cleary, M.P., *Rev. Geophys.*, 12, 227-241, 1976.